12

EDGEWOOD
RESEARCH, DEVELOPMENT & ENGINEERING CENTER
U.S. ARMY CHEMICAL AND BIOLOGICAL DEFENSE COMMAND

ERDEC-TR-215

SCREENING SMOKE PERFORMANCE OF COMMERCIALLY AVAILABLE POWDERS

III. INFRARED AND VISIBLE SCREENING BY CARBON BLACK

Janon F. Embury

RESEARCH AND TECHNOLOGY DIRECTORATE

Donald L. Walker
Curtis J. Zimmermann

GEO-CENTERS, INC.
Fort Washington, MD 20744

November 1994

CUM SCIENTIA DEFENDIMUS

Approved for public release; distribution is unlimited.

Aberdeen Proving Ground, MD 21010-5423

Disclaimer

REPORT DOCUMENTATION PAGE	Form Approved OMB No. 0704-0188

1. AGENCY USE ONLY *(Leave blank)*	2. REPORT DATE	3. REPORT TYPE AND DATES COVERED
	1994 November	Final, 91 Aug - 93 Feb

4. TITLE AND SUBTITLE
Screening Smoke Performance of Commercially Available Powders; III. Infrared and Visible Screening by Carbon Black

5. FUNDING NUMBERS
PR-10464609D200

6. AUTHOR(S)
Embury, Janon F. (ERDEC); Walker, Donald L.; and Zimmermann, Curtis J. (GEO-CENTERS, INC.)

7. PERFORMING ORGANIZATION NAME(S) AND ADDRESS(ES)
DIR, ERDEC,* ATTN: SCBRD-RTB, APG, MD 21010-5423

GEO-CENTERS, INC., Fort Washington, MD 20744

8. PERFORMING ORGANIZATION REPORT NUMBER
ERDEC-TR-215

9. SPONSORING/MONITORING AGENCY NAME(S) AND ADDRESS(ES)

10. SPONSORING/MONITORING AGENCY REPORT NUMBER

11. SUPPLEMENTARY NOTES
*When this study was conducted, ERDEC was known as the U.S. Army Chemical Research, Development and Engineering Center and the author was assigned to the Research Directorate.

12a. DISTRIBUTION/AVAILABILITY STATEMENT
Approved for public release; distribution is unlimited.

12b. DISTRIBUTION CODE

13. ABSTRACT *(Maximum 200 words)*

This is the third in a series of reports that evaluate the smoke screening performance of commercially available powders. The first report described performance parameters and developed figures of merit to compare the ability of smoke materials, to attenuate electromagnetic radiation in the visible infrared and microwave spectral regions. This report investigates carbon black pigments. Many of them attenuate visible radiation better than titanium dioxide described in the second report and a few of them attenuate infrared radiation better than graphite flake described in the first report of the series. Coagulation leads to the formation of large carbon black chain aggregates which govern the screening properties. An additional criterion, contrast reduction, must be included when comparing a white visible screening smoke such as titanium dioxide with a black visible screening material such as carbon black. Results from modeling the contrast transmittance of white and black smokes indicate that the tabulated carbon black figures of merit based on attenuation of radiation should be divided by 1.5 to compare its contrast reduction capability with that of a white smoke.

14. SUBJECT TERMS

Visible screening	Obscurants	Smoke
Infrared screening	Carbon black	Contrast
Powders technology	Figures of merit	Coagulation

15. NUMBER OF PAGES
23

16. PRICE CODE

17. SECURITY CLASSIFICATION OF REPORT	18. SECURITY CLASSIFICATION OF THIS PAGE	19. SECURITY CLASSIFICATION OF ABSTRACT	20. LIMITATION OF ABSTRACT
UNCLASSIFIED	UNCLASSIFIED	UNCLASSIFIED	UL

Blank

PREFACE

The work described in this report was authorized under Project No. 10464609D200, Screening Smoke Materiel Engineering. This work was started in August 1991 and completed in February 1993.

The use of trade names or manufacturers' names in this report does not constitute an official endorsement of any commercial products. This report may not be cited for purposes of advertisement.

This report has been approved for release to the public. Registered users should request additional copies from the Defense Technical Information Center, unregistered users should direct such requests to the National Technical Information Service.

Accesion For

NTIS CRA&I
DTIC TAB
Unannounced
Justification

By
Distribution /

Availability Codes

Dist	Avail and / or Special
A-1	

Blank

CONTENTS

FIGURES

TABLE

SCREENING SMOKE PERFORMANCE OF COMMERCIALLY AVAILABLE POWDERS

III. INFRARED AND VISIBLE SCREENING BY CARBON BLACK

INTRODUCTION

Some carbon black extinction coefficients in the visible spectral region are superior to any other screening material, however not all of the carbon blacks with superior extinction coefficients are expected to perform as well as titania, WP or even fog oil because a black smoke takes minimal advantage of glare (path radiance) which significantly assists screening. Radiative transfer calculations[1] comparing contrast transmittance and perceived lightness transmittance through a carbon black versus a white smoke, such as titania, indicate that optical depth of the carbon black smoke would have to be about 1.5 times greater than that of the titania white smoke for equivalent screening performance. In other words when the extinction coefficient of the carbon black in the visible region exceeds the extinction coefficient of the titania by more than a factor of 1.5 we can expect the carbon black to be superior to titania for visible screening. Visible screening comparisons with titania[2] can be made simply by dividing all carbon black figures of merit by 1.5. Similar comparison can be made with fog oil and white phosphorus but in the case of white phosphorus the low humidity yield factor of approximately 3 should be multiplied by the extinction coefficient for the comparison.

Judging from the performance parameters[3] that have been measured in the ERDEC smoke chamber for a variety of commercial carbon black pigment samples, the weight limited figure of merit[3] of all other powder obscurants would probably be improved in the near infrared (1.06μm) by the addition of carbon black. The volume limited figure of merit of other powder obscurants would probably be improved in not only the near infrared but also the mid (3-5μm) and far (8-14μm) infrared because carbon black primary particles are small enough to fill the interstitial void volume of packed powders containing much larger particles that constitute other screening materials. The carbon black particles have an added advantage in that they may assist in deagglomeration of compressed screening powder mixtures. Their 10-20 nanometer primary particle diameter provides a standoff distance limiting the surface area of contact and van der Waals forces among larger particles without significant reductions in packing density. In fact any small reduction in packing density due to this effect would probably be more than offset by a significant increase in packing density due to filling of the large particle interstitial void volume and an increase in dissemination yield.

COAGULATION OF SOOT AEROSOLS

Carbon "soot" aerosols consist of aggregates of roughly spherical primary particles with diameters $D \approx 10^{-6}$ cm on the order of ten nanometers and primary particle densities of $\rho \approx 1.86 g/cm^3$. Coagulation of such small primary particles can be expected to occur rapidly at mass concentrations $C_m \approx 0.1 g/m^3$ typical of smoke chamber testing because of the large initial t=0 number concentrations C_N:

$$C_N(t=0)=\frac{C_M(t=0)}{\rho\frac{\pi}{6}D^3}=\frac{(0.1g/m^3)(10^{-6}m^3/cm^3)}{(1.86g/cm^3)(\frac{\pi}{6})(10^{-6}cm)^3}=1.03X10^{11}/cm$$

To get an idea of the magnitude of the effect we have for Brownian (thermal) coagulation of a monodisperse aerosol with constant coagulation coefficient K

$$C_N(t)=\frac{C_N(t=0)}{1+C_N(t=0)\frac{\mathrm{K}t}{2}}$$

the number concentration as a function of time t, initial number concentration $C_N(t=0)$ and coagulation coefficient K. The coagulation coefficient may be expressed in terms of the air temperature T, viscosity η and Cunningham slip correction factor C_c

$$\mathrm{K}=\frac{8}{3}\frac{kT}{\eta}C_c$$

where k is the Boltzman constant ($1.38X10^{-16}$erg/^{o}K) and

$$C_c=1+\frac{2\lambda}{D}[1.257+0.40e^{-1.1\frac{D}{2\lambda}}]$$

where $\lambda\approx 0.07\mu m$ is the air molecule mean free path under standard temperature and pressure. For carbon primary particles at ambient temperature T=293^{o}K and $\eta=1.83X10^{-4}$g/cm-sec, we find that $C_c\approx 23.8$ and

$$\mathrm{K}=\frac{8}{3}\frac{(1.38X10^{-16})(293)}{1.83X10^{-4}}(23.8)=1.40X10^{-8}cm^3/\sec$$

so that an initial number concentration of $10^{11}/cm^3$ of primary particles will be reduced in one second to a number concentration of aggregates equal to

$$C_N(t=1\sec)=\frac{10^{11}/cm^3}{1+\frac{(10^{11})(1.4X10^{-8})}{2}}\approx 1.43X10^8/cm^3$$

with an average number of $\approx$1000 primary particles/aggregate. In fact, however the Cunningham slip correction factor representing the aggregate takes on values less than 23.8, that of a primary single particle. Therefore the coagulation coefficient of the aggregate can be as small as 1/23.8 that of the primary particles. Using this lower value for the coagulation coefficient we can predict a lower limit aggregate size at an upper limit number concentration. We find that after one second aggregates will contain approximately $40\leq N\leq 1000$

primary particles in chains. Depending on how quickly number concentration is reduced during the pneumatic powder dissemination process, this number of particles per aggregate could be even higher. For example, if turbulent shear became low enough near the dissemination source for coagulation to dominate deaggregation in the disseminator for one hundredth of a second, at concentrations more than one hundred times greater than the chamber concentration, we would expect bigger aggregates.

EXTINCTION SPECTRA OF SOOT AGGREGATES

Carbon black aggregates have much higher extinction coefficients in all the wavelength bands considered compared to primary carbon black particles. Because primary particle diameters are much smaller than the wavelengths in the spectral regions considered, we can interpret this in terms of the Rayleigh spheroid low frequency electromagnetic scattering theory. Both prolate and oblate spheroidal shaped carbon aggregates have higher extinction coefficients in the visible and IR than the roughly spherical primary particles. If conductive chain aggregates of primary particles are modeled as distributions of prolate spheroidal shapes, we predict extinction spectra as indicated in Figure 1 with a reference measured curve found by averaging a number of carbon black spectra. The refractive index data was obtained from the ERDEC data base for soot[4]. If modeled as low density fluffy spherical aggregates we use the Mie Theory to calculate the extinction spectra shown in Figure 2 where mass median diameter (MMD) is specified in micrometers. Computed spectra should be multiplied by the reciprocal void volume fraction for a better match with the chamber measurements of an average carbon black sample. Although we might expect void volume fractions of soot aggregates to be smaller, a spectral approximate match in extinction coefficients is obtained at a void volume fraction somewhat greater than 1/2 at the optimum diameter of approximately 0.8μm. Adjustments in mass median aspect ratio and sigma G do not improve the longer wavelength match in the spectra appearing in Figure 1; the shorter wavelength mismatch is because we are beyond the region of applicability of the low frequency theory. We might match measurements better with model predictions, whether fluffy sphere or prolate spheroid, by adjusting the effective complex refractive index due to surface contact resistance between primary particles.

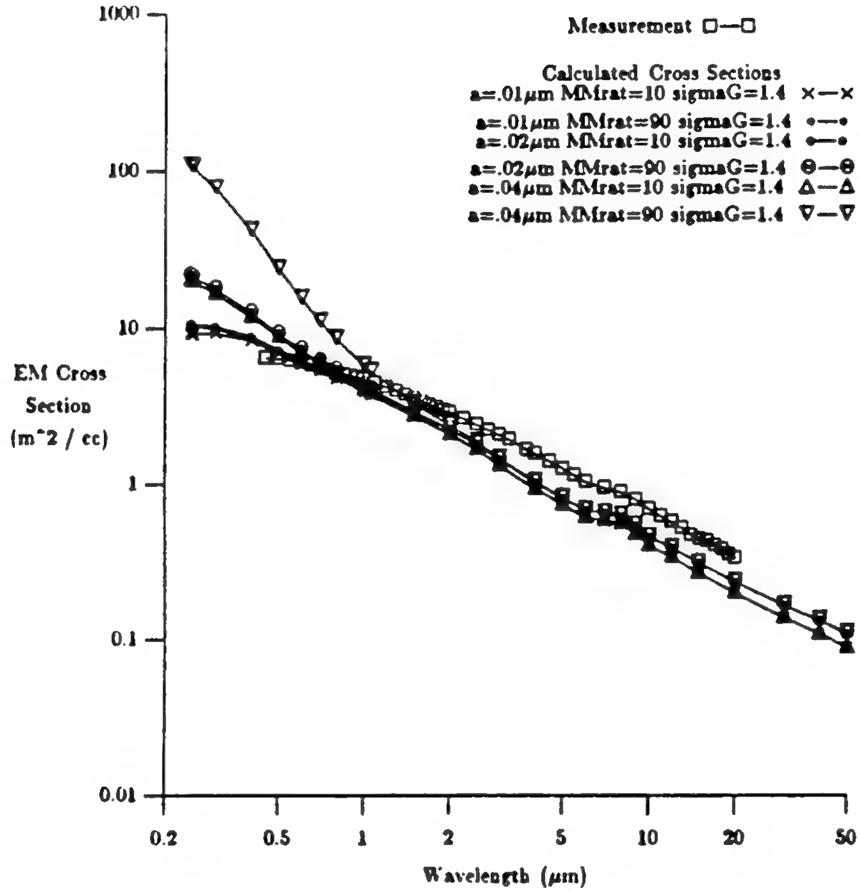

Figure 1. Log Normal Size Distributions of Chains of Monodisperse Carbon Particle Cross Sections Predicted Using the Rayleigh Low Frequency Theory for Prolate Spheriods with Equatorial Semi-axis 'a' and a Mass Median Aspect Ratio 'MMrat' with a Geometric Standard Deviation 'sigmaG'

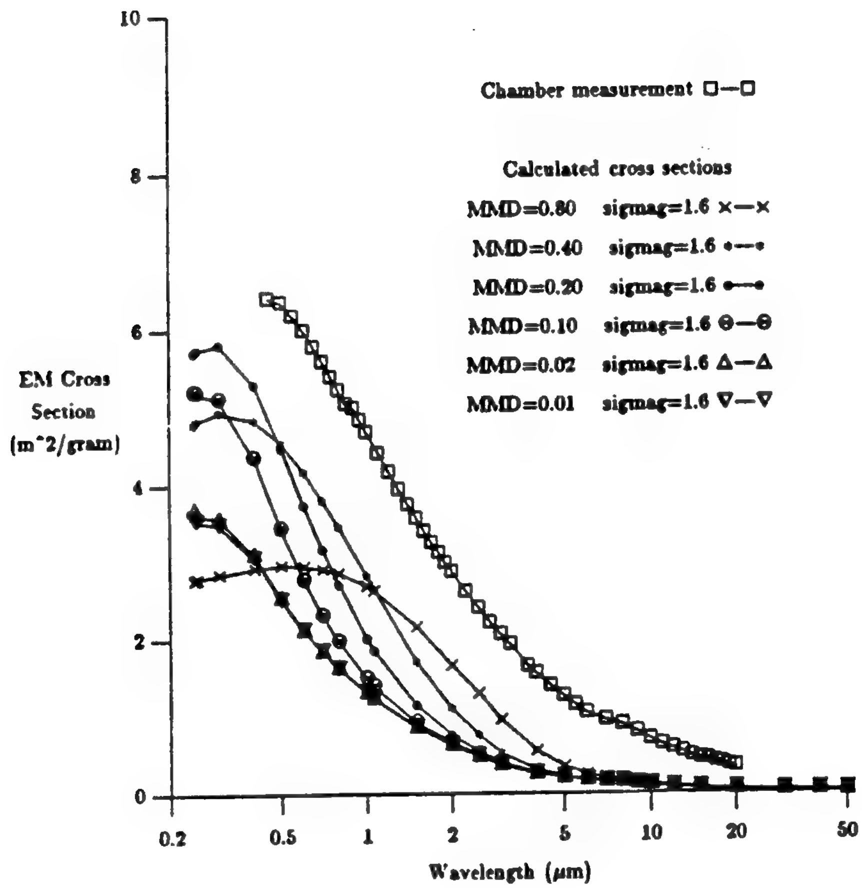

Figure 2. Extinction Coefficient Spectra of Carbon (Soot) Aerosol Cross Sections Calculated by Averaging over Log Normal Size Distributions of Spherical Particles

CARBON BLACK MANUFACTURING

Carbon black is one of the most widely used black pigments in the coatings industry. It provides pigmentation, conductivity and UV resistance to a wide range of products. The fine particulate pigment material is produced by the combustion or thermal decomposition of hydrocarbon compounds. The different methods of production (variations in process control conditions and feed stock) will determine the characteristics of the carbon black and thus produce wide varieties of the pigment. Raw materials used for pigment production are petroleum or liquid coal tar hydrocarbons, natural gas and acetylene. Depending on the feed stock, one can produce the different blacks known as lamp black, bone black, channel black, acetylene black, and furnace black. For military obscuration the generic terminology of "carbon black" will be used.

Petroleum products and coal tar products serve as the primary feed stock for carbon black production. Some specialized carbon blacks are produced from the exothermic decomposition of acetylene yielding high purity carbon black having a carbon content as high as 99.5%. A typical production sequence for a furnace black produced from an aromatic petroleum distillate feed stock could be described as follows. The feed stock is atomized into a stream of combustion gases at high velocity essentially cracking the petroleum feed stock to produce carbon black and hydrogen. Reaction temperature, residence time and carbon content of the feed stock all effect the yield and final structure of the carbon black. Thermal black production is based on natural gas feed stocks which undergo high temperature decomposition in the absence of air or flames. Such reactions for thermal black production are highly endothermic and thus are very energy intensive. The majority of production methods result in aggregated particles consisting of primary particles generally in the nanometer size range. In all cases of production it is possible to vary particle size, aggregate size and surface chemistry by controlled manipulation of reactor conditions.

ERDEC SMOKE CHAMBER MEASUREMENTS

The 14 cubic meter ERDEC smoke chamber used to measure the performance parameters such as the electromagnetic extinction cross section per mass of aerosol (α), yield (Y) and deposition velocity (υ_D) was described in the first series of these reports[3]. Glass fiber filters, a rotometer and vacuum pump are used to make aerosol concentration measurements at a flow rate of 20 liters per minute. A photodiode array spectrometer measures aerosol transmittance over the wavelength range of 0.4µm-1.0µm. Two FTIR spectrometers measure aerosol transmittance over the spectral regions 0.9µm-3µm and 2.5µm-22µm. At concentrations below a few milligrams of aerosol per cubic meter of air a quartz crystal microbalance (QCM) and an aerodynamic particle sizer (APS) measure aerodynamic particle size distribution. A Stanford Research Institute sonic pneumatic nozzle is operated at 60 psi to disperse and deaggregate powders to produce an aerosol. A mixing fan is operated continuously in the chamber at a low speed to maintain uniform concentration

and provide a level of turbulence driving reaerosolization and impaction approximating those components of aerosol deposition in the battlefield. Measurements of root mean square air velocity fluctuations could have been made and compared with typical turbulance energy dissipation rates of $1000 cm^2/sec^3$ at a height of 1 meter above the ground[5], but instead a mixing fan speed was chosen that produced a homogeneous cloud within a few seconds after dissemination was completed and where expected variations in fan speed do not seem to significantly affect deposition rates. The aerosol sedimentation component of deposition will of course be independent of whether the aerosol is in a chamber or on the battlefield.

CONCLUSION

The concept of describing competing smoke materials in terms of four measured performance parameters (extinction coefficient α, dissemination yield Y, deposition velocity υ_D, and powder packing density ρ) has been presented and three figures of merit based on the four performance parameters have been introduced in the first report[3] of this series. All three figures of merit are proportional to smoke plume optical depth downwind and can be used not only to rank performance, but also quantitatively to predict cloud plume opacities downwind. The first figure of merit gives the square meters of smoke screening per mass of smoke material transported and is useful in weight limited applications such as large area smoke generators. The second figure of merit gives the square meters of screening per volume of smoke material transported and is useful in volume limited applications such as grenades, rockets, artillery rounds, mortars and smoke pots. The third figure of merit gives the square meters of screening per dollar of smoke material cost. Here for example the weight constraint of the large area smoke generator vehicle would have to be met first by specifying a minimum value for the first figure of merit (weight limited) and then comparing all materials satisfying this constraint based on the third figure of merit (financial limited).

A brief summary of the carbon black manufacturing process was given. Testing these materials in the ERDEC smoke chamber to obtain dissemination yield Y, deposition velocity υ_D and spectral extinction coefficient α from the visible through $20 \mu m$ wavelength was also described along with a description of the coagulation process that accompanies such measurements.

Single primary particle spectra would not be expected due to the large number concentrations. Instead we expect dendritic chains of primary particles or larger roughly spherical fluffy aggregates. Methods for interpreting the measured extinction coefficient spectra of aggregates were proposed. The Rayleigh ellipsoidal theory and the Mie theory were used to compute results based on these two aggregate conceptualizations. Computed results generally fell below measured results which points towards the need to obtain more representative refractive index values for dendritic and spherical clusters of primary particles.

A wide variety of carbon black powders have been tested in the ERDEC smoke chamber using the SRI sonic pneumatic nozzle at a pressure of 60 psi for dissemination. Performance parameters and their figures of merit are

tabulated in Table 1 so that materials can be compared over the visible, 1.06μm, 3-5μm and 8-14μm spectral regions. The volume limited figure of merit is calculated based on the particle density of 1.86g/cm^3 rather than a packed powder density because of variability in the packing density and because the particle density represents an upper limit to the packing density. Carbon black can potentially screen better than any other powder material in the near infrared (1.06μm). For volume limited applications carbon black can be mixed with other screening powder materials with virtually no increase in volume because the particles are small enough to fill the interstitial void volume among larger screening particles. It can also improve grinding/dissemination yields when mixed with other materials by limiting adhesion forces among larger particles.

REFERENCES

1. Embury, J.F., Walker, D., and Zimmermann, C.J., "Screening Smoke Performance of Commercially Available Powders II Visible Screening by Titanium Dioxide," ERDEC-TR-168, APG, MD, June 1994.

2. Embury, J.F., Walker, D., and Zimmermann, C.J., "Screening Smoke Performance of Commercially Available Powders I Infrared Screening by Graphite Flake," ERDEC-TR-093, APG, MD, July 1993.

3. Querry, M.R., "Optical Constants of Minerals and Other Materials from the Millimeter to the Ultraviolet," CRDEC-CR-88009, APG, MD, 1987.

4. Friedlander, S.K., Smoke, Dust and Haze, John Wiley and Sons, New York, NY, November 1977.

5. Embury, J.F., "White, Black, Emissive and One Smoke and Radar Scattering and Absorbing Smokes," to be Submitted for Publication in Applied Optics.

PERFORMANCE PARAMETERS AND FIGURES OF MERIT
FOR VISIBLE AND INFRARED SCREENING CARBON BLACK MATERIALS
CHAMBER TESTS UTILIZING SRI NOZZLE AT 60 PSI¶

TABLE 1

MATERIAL AND COST§ 10.6.5/4.23/3.10.26	BET SURFACE AREA (m^2/g)	PARTICLE DENSITY $\rho(g_d/cm^3)$	YIELD $Y(g_a/g_d)$	DEPOSITION VELOCITY V_D(cm/sec)	AVG ALPHA $\alpha(m^2/g_a)$ 0.45-0.65μm 1.06μm 3.0-5.0μm 8.0-14.0μm	AVG ALPHA*RHO $\alpha*\rho$ (m^2/cm^3)	WEIGHT LIMITED FIGURE OF MERIT $\Phi_W=\alpha*Y$ (m^2/g_d)	VOLUME LIMITED FIGURE OF MERIT $\Phi_V=\alpha*Y*\rho$ (m^2/cm^3)	FINANCIAL LIMITED FIGURE OF MERIT $\Phi_F=\alpha*Y/COST$ ($m^2/\$$)†
ASBURY 5305 @≈ \$0.30/lb ≈2,000 lb	≈40	1.86	0.816	0.153	4.52 3.36 1.17 0.60	8.41 6.25 2.18 1.12	3.69 2.74 0.96 0.49	6.86 5.10 1.78 0.91	5,584 4,146 1,452 741
CABOT 250 @≈ \$0.76/lb	≈50	1.86	0.172	0.259	2.08 1.72 1.13 0.80	3.87 3.20 2.10 1.49	0.36 0.30 0.19 0.14	0.67 0.55 0.36 0.26	215 179 113 83
CABOT 250R @≈ \$0.82/lb	≈50	1.86	0.851	0.143	2.71 2.33 1.41 0.86	5.04 4.33 2.62 1.60	2.31 1.98 1.20 0.73	4.29 3.69 2.23 1.36	1,278 1,096 664 404

TABLE 1 CONTINUED

MATERIAL AND COST§ 10.6.5/4.23/3.10.26	BET SURFACE AREA (m^2/g)	PARTICLE DENSITY $\rho(g_d/cm^3)$	YIELD $Y(g_a/g_d)$	DEPOSITION VELOCITY V_D(cm/sec)	AVG ALPHA $\alpha(m^2/g_a)$ 0.45-0.65μm 1.06μm 3.0-5.0μm 8.0-14.0μm	AVG ALPHA*RHO $\alpha*\rho$ (m^2/cm^3)	WEIGHT LIMITED FIGURE OF MERIT $\Phi_W=\alpha*Y$ (m^2/g_d)	VOLUME LIMITED FIGURE OF MERIT $\Phi_V=\alpha*Y*\rho$ (m^2/cm^3)	FINANCIAL LIMITED FIGURE OF MERIT $\Phi_F=\alpha*Y/COST$ ($m^2/\$$)†
CABOT BLACK PEARLS 700 @≈ $1.28/lb	≈200	1.86	0.430	0.159	3.76 2.98 1.65 0.98	6.99 5.54 3.07 1.82	1.61 1.28 0.71 0.42	3.01 2.38 1.32 0.78	619 492 273 161
CABOT MONARCH 700 @≈ $1.28/lb	≈200	1.86	0.968	0.085	4.21 3.53 1.96 1.05	7.83 6.57 3.65 1.95	4.08 3.42 1.90 1.02	7.58 6.36 3.53 1.89	1,447 1,213 673 361
CABOT MONARCH 900 @≈ $1.75/lb	≈230	1.86	0.942	0.065	3.34 3.06 1.97 0.95	6.21 5.69 3.66 1.77	3.15 2.88 1.85 0.89	5.85 5.36 3.45 1.66	817 747 479 230
CABOT MONARCH 1300 @≈ $4.83/lb	≈560	1.86	0.849	0.177	2.36 2.05 1.26 0.73	4.39 3.81 2.34 1.36	2.00 1.74 1.07 0.62	3.73 3.24 1.99 1.15	188 163 100 58
CABOT MONARCH 1400 @≈ $6.03/lb	≈560	1.86	0.882	0.170	2.23 1.99 1.26 0.73	4.15 3.70 2.34 1.36	1.97 1.76 1.11 0.64	3.66 3.26 2.07 1.20	148 132 83 48
COLUMBIA RAVEN 850 B @≈ $0.62/lb ≈2,500 lb	≈70	1.86	0.228	0.205	4.22 2.96 1.27 0.73	7.85 5.51 2.36 1.36	0.96 0.68 0.29 0.17	1.79 1.26 0.54 0.31	702 497 212 124
COLUMBIA RAVEN 1020 B @≈ $0.62/lb ≈2,500 lb	≈95	1.86	0.157	0.343	1.94 1.68 1.12 0.77	3.61 3.13 2.08 1.43	0.31 0.26 0.18 0.12	0.57 0.49 0.33 0.23	227 190 131 87

TABLE 1 CONTINUED

MATERIAL AND COST[§] 10.6.5/4.23/3.10.26	BET SURFACE AREA (m^2/g)	PARTICLE DENSITY $\rho(g_d/cm^3)$	YIELD $Y(g_a/g_d)$	DEPOSITION VELOCITY V_D(cm/sec)	AVG ALPHA $\alpha(m^2/g_a)$ 0.45-0.65μm 1.06μm 3.0-5.0μm 8.0-14.0μm	AVG ALPHA*RHO $\alpha*\rho$ (m^2/cm^3)	WEIGHT LIMITED FIGURE OF MERIT $\Phi_W=\alpha*Y$ (m^2/g_d)	VOLUME LIMITED FIGURE OF MERIT $\Phi_V=\alpha*Y*\rho$ (m^2/cm^3)	FINANCIAL LIMITED FIGURE OF MERIT $\Phi_F=\alpha*Y/COST$ ($m^2/\$$)[†]
COLUMBIA RAVEN 1170 P @≈ $0.77/lb ≈2,000 lb	≈120	1.86	0.866	0.115	3.02 2.55 1.51 0.87	5.62 4.75 2.81 1.62	2.62 2.21 1.31 0.75	4.87 4.11 2.44 1.40	1,544 1,303 772 442
COLUMBIA RAVEN 1255 B @≈ $1.06/lb ≈2,500 lb	≈125	1.86	0.237	0.275	2.29 1.86 1.12 0.72	4.26 3.46 2.08 1.34	0.54 0.44 0.26 0.17	1.01 0.82 0.49 0.32	231 188 111 72
COLUMBIA RAVEN 2000 B @≈ $1.01/lb ≈2,500 lb	≈190	1.86	0.444	0.302	1.74 1.59 1.11 0.75	3.24 2.96 2.07 1.40	0.77 0.71 0.50 0.33	1.44 1.31 0.92 0.62	346 319 224 148
COLUMBIA RAVEN 5000 B @≈ $4.55/lb ≈2,500 lb	≈430	1.86	0.340	0.281	1.97 1.75 1.13 0.69	3.66 3.25 2.10 0.23	0.67 0.60 0.38 0.24	1.25 1.11 0.72 0.44	66 59 37 23
COLUMBIA RAVEN 5000 P @≈ $4.65/lb ≈2,000 lb	≈430	1.86	0.532	0.168	2.21 1.96 1.22 0.67	4.10 3.65 2.27 1.24	1.17 1.04 0.65 0.35	2.18 1.94 1.21 0.66	114 101 63 34
COLUMBIA RAVEN 5750 P @≈ $4.31/lb ≈2,000 lb	≈575	1.86	0.882	0.143	2.48 2.23 1.41 0.75	4.61 4.14 2.62 1.40	2.18 1.96 1.24 0.67	4.06 3.65 2.31 1.24	229 206 130 70

TABLE 1 CONTINUED

MATERIAL AND COST§ 10.6.5/4.23/3.10.26	BET SURFACE AREA (m^2/g)	PARTICLE DENSITY $\rho(g_d/cm^3)$	YIELD $Y(g_a/g_d)$	DEPOSITION VELOCITY V_D(cm/sec)	AVG ALPHA $\alpha(m^2/g_a)$ 0.45-0.65μm 1.06μm 3.0-5.0μm 8.0-14.0μm	AVG ALPHA*RHO $\alpha*\rho$ (m^2/cm^3)	WEIGHT LIMITED FIGURE OF MERIT $\Phi_W=\alpha*Y$ (m^2/g_d)	VOLUME LIMITED FIGURE OF MERIT $\Phi_V=\alpha*Y*\rho$ (m^2/cm^3)	FINANCIAL LIMITED FIGURE OF MERIT $\Phi_F=\alpha*Y/COST$ ($m^2/\$$)†
COLUMBIA CONDUCTEX 975 @≈ $1.10/lb ≈10,000 lb	≈250	1.82	0.497	0.112	6.53 4.90 1.98 0.99	11.89 8.91 3.60 1.80	3.25 2.44 0.98 0.49	5.09 4.43 1.79 0.89	1,339 1,005 406 203
COLUMBIA CONDUCTEX SC B @≈ $0.89/lb ≈2,000 lb	≈220	1.82	0.545	0.153	5.05 3.51 1.60 0.92	9.19 6.39 2.91 1.67	2.75 1.91 0.87 0.50	5.09 3.48 1.59 0.91	1,402 974 443 255
COLUMBIA CONDUCTEX SC P @≈ 0.94/lb ≈2,000 lb	≈220	1.86	0.999	0.062	5.96 4.39 1.91 0.94	11.08 8.17 3.56 1.74	5.95 4.39 1.91 0.93	11.07 8.16 3.56 1.74	2,873 2,120 922 449
DEGUSSA PRINTEX L @ $1.40/lb ≈22,000 lb	≈265	1.86	1.00	0.056	6.55 4.71 1.97 0.97	12.18 8.76 3.66 1.80	6.55 4.71 1.97 0.97	12.18 8.76 3.66 1.80	2,124 1,527 638 314
DEGUSSA PRINTEX L6 @ $1.40/lb ≈22,000 lb	≈150	1.86	0.921	0.064	5.23 4.13 2.02 1.04	9.73 7.68 3.76 1.93	4.82 3.80 1.86 0.96	8.96 7.07 3.46 1.78	1,563 1,232 603 311
DEGUSSA PRINTEX P B @≈ $0.99/lb ≈2,300 lb	≈120	1.86	0.555	0.182	5.23 3.59 1.55 0.89	9.72 6.68 2.88 1.66	2.90 2.00 0.86 0.49	5.40 3.71 1.60 0.92	1,329 917 394 224

TABLE 1 CONTINUED

MATERIAL AND COST§ 10.6.5/4.23/3.10.26	BET SURFACE AREA (m^2/g)	PARTICLE DENSITY $\rho(g_d/cm^3)$	YIELD $Y(g_a/g_d)$	DEPOSITION VELOCITY V_D(cm/sec)	AVG ALPHA $\alpha(m^2/g_a)$ 0.45-0.65μm 1.06μm 3.0-5.0μm 8.0-14.0μm	AVG ALPHA*RHO $\alpha*\rho$ (m^2/cm^3)	WEIGHT LIMITED FIGURE OF MERIT $\Phi_W=\alpha*Y$ (m^2/g_d)	VOLUME LIMITED FIGURE OF MERIT $\Phi_V=\alpha*Y*\rho$ (m^2/cm^3)	FINANCIAL LIMITED FIGURE OF MERIT $\Phi_F=\alpha*Y/COST$ ($m^2/\$$)†
DEGUSSA PRINTEX V @≈ $1.65/lb ≈1,200 lb	≈100	1.86	0.835	0.060	5.93 4.31 1.54 0.70	11.03 8.02 2.86 1.30	4.95 3.60 1.29 0.58	9.21 6.70 2.39 1.09	1,362 990 354 159
DEGUSSA PRINTEX X_{E2} @≈ $3.77/lb ≈600 lb	≈1000	1.86	0.205	0.191	3.47 3.09 2.07 1.45	6.45 5.75 3.85 2.70	0.71 0.63 0.42 0.30	1.32 1.18 0.79 0.55	85 75 50 36
DEGUSSA PRINTEX 55 @≈ $1.04/lb ≈1,400 lb	≈110	1.86	0.755	0.116	2.66 2.49 1.67 0.93	4.95 4.63 3.11 1.73	2.06 1.93 1.29 0.72	3.83 3.59 2.41 1.34	899 842 563 314
DEGUSSA F 101 @≈ $0.99/lb ≈2,000 lb	≈20	1.86	0.969	0.024	4.92 4.85 2.63 1.14	9.15 9.02 4.89 2.12	4.77 4.70 2.55 1.10	8.87 8.74 4.74 2.05	2,187 2,155 1,169 504
DEGUSSA FW 200 @≈ $1.91/lb ≈1,000 lb	≈460	1.86	0.999	0.146	2.99 2.72 1.43 0.66	5.56 5.06 2.66 1.23	2.99 2.72 1.43 0.66	5.56 5.05 2.66 1.23	710 646 339 156
DEGUSSA S-BLACK 4A @≈ $2.25/lb ≈1,600 lb	≈180	1.86	0.749	0.135	4.29 2.99 1.18 0.62	7.98 5.56 2.19 1.15	3.21 2.24 0.88 0.46	5.98 4.16 1.64 0.86	647 451 177 92
DEGUSSA S-BLACK 100 @≈ $1.76/lb ≈1,200 lb	≈30	1.86	0.927	0.049	4.93 4.25 2.08 1.00	9.17 7.91 3.87 1.86	4.57 3.94 1.93 0.97	8.50 7.33 3.59 1.72	1,178 1,016 497 250

TABLE 1 CONTINUED

MATERIAL AND COST§ 10.6.5/4.23/3.10.26	BET SURFACE AREA (m^2/g)	PARTICLE DENSITY $\rho(g_d/cm^3)$	YIELD $Y(g_a/g_d)$	DEPOSITION VELOCITY V_D(cm/sec)	AVG ALPHA $\alpha(m^2/g_a)$ 0.45-0.65μm 1.06μm 3.0-5.0μm 8.0-14.0μm	AVG ALPHA*RHO $\alpha*\rho$ (m^2/cm^3)	WEIGHT LIMITED FIGURE OF MERIT $\Phi_W=\alpha*Y$ (m^2/g_d)	VOLUME LIMITED FIGURE OF MERIT $\Phi_V=\alpha*Y*\rho$ (m^2/cm^3)	FINANCIAL LIMITED FIGURE OF MERIT $\Phi_F=\alpha*Y/COST$ ($m^2/\$$)†
DEGUSSA S-BLACK 550 @≈ \$1.52/lb ≈1,400 lb	≈110	1.86	0.929	0.084	3.18 2.80 1.74 0.89	5.91 5.21 3.24 1.65	2.95 2.60 1.62 0.83	5.49 4.84 3.01 1.54	881 776 483 247
EBONEX COSMIC D-2 @≈ \$0.68/lb ≈1,000 lb		2.52	0.898	0.110	1.66 1.22 0.38 0.21	4.18 3.07 0.96 0.53	1.49 1.10 0.96 0.53	3.76 2.76 0.86 0.48	994 734 640 353
HUBER N220 @≈ \$0.42/lb ≈45,000 lb	≈119	1.86	0.232	0.242	4.26 2.91 1.26 0.73	7.92 5.41 2.34 1.35	0.98 0.68 0.29 0.17	1.84 1.26 0.54 9.31	1,059 735 313 183
HUBER N375 @≈ \$0.39/lb ≈45,000 lb	≈100	1.86	0.211	0.164	4.81 3.20 1.30 0.75	8.95 5.95 2.41 1.39	1.02 0.67 0.27 0.16	1.89 1.26 0.51 0.29	1,187 779 314 186
HUBER S212 @≈ \$0.63/lb ≈45,000 lb	≈117	1.86	0.255	0.233	3.53 2.57 1.25 0.75	6.57 4.78 2.33 1.40	0.90 0.66 0.32 0.19	1.64 1.22 0.59 0.35	648 475 230 136
SID RICHARDSON N110 @≈ \$0.43/lb ≈2,500 lb	≈144	1.86	0.269	0.217	4.07 2.90 1.38 0.83	7.58 5.39 2.58 1.54	1.10 0.78 0.37 0.22	2.04 1.45 0.69 0.42	1,161 823 390 232

TABLE 1 CONTINUED

MATERIAL AND COST§ 10.6.5/4.23/3.10.26	BET SURFACE AREA (m^2/g)	PARTICLE DENSITY $\rho(g_d/cm^3)$	YIELD $Y(g_a/g_d)$	DEPOSITION VELOCITY V_D(cm/sec)	AVG ALPHA $\alpha(m^2/g_a)$ 0.45-0.65μm 1.06μm 3.0-5.0μm 8.0-14.0μm	AVG ALPHA*RHO $\alpha*\rho$ (m^2/cm^3)	WEIGHT LIMITED FIGURE OF MERIT $\Phi_W=\alpha*Y$ (m^2/g_d)	VOLUME LIMITED FIGURE OF MERIT $\Phi_V=\alpha*Y*\rho$ (m^2/cm^3)	FINANCIAL LIMITED FIGURE OF MERIT $\Phi_F=\alpha*Y/COST$ ($m^2/\$$)†
SID RICHARDSON N134 @≈ $0.47/lb ≈2,500 lb		1.86	0.209	0.194	4.39 3.03 1.39 0.82	8.16 5.63 2.58 1.53	0.92 0.63 0.29 0.17	1.71 1.18 0.54 0.32	888 608 280 164
SID RICHARDSON N135 @≈ $0.43/lb ≈2,500 lb		1.86	0.215	0.135	5.79 3.84 1.60 0.90	10.76 7.14 2.97 1.67	1.24 0.82 0.34 0.19	2.31 1.53 0.64 0.36	1,309 865 358 2000
SID RICHARDSON N234 @≈ $0.40/lb ≈2,500 lb	≈122	1.86	0.169	0.161	5.14 3.47 1.49 0.86	9.56 6.46 2.78 1.60	0.87 0.59 0.25 0.15	1.62 1.09 0.47 0.27	987 669 283 170
SID RICHARDSON N343 @≈ $0.36/lb ≈2,500 lb	≈96	1.86	0.169	0.175	5.53 3.69 1.48 0.82	10.29 6.86 2.75 1.53	0.93 0.62 0.25 0.14	1.74 1.16 0.46 0.26	1,172 781 315 176
SID RICHARDSON N358 @≈ $0.36/lb ≈2,500 lb	≈82	1.86	0.231	0.160	5.73 3.85 1.48 0.82	10.66 7.17 2.76 1.52	1.32 0.89 0.34 0.19	2.46 1.65 0.64 0.35	1,664 1,122 428 239

AVERAGE ALPHA VALUES SELECTED FOR THE FOLLOWING REASONS:

0.45-0.65μm visible light corresponds to the range of maximum photopic and scotopic response for the human eye. An unweighted average was choosen because of the differences between these responses and variability in natural illumination spectra.

1.06μm is the operating wavelength of neodinium YAG laser designators.

3.0-5.0μm is the operating regime for thermal imaging systems that rely on indium antimonide detectors. An unweighted average was choosen because of variability in source temperature and spectral emissivity.

8.0-14.0μm is the operating regime for thermal imaging systems that rely on mercury cadmium telluride detectors. An unweighted average was choosen because of variability in source temperature and spectral emissivity.

g_a=grams aerosol, g_d=grams disseminated=grams transported

† (\$/lb)(lb/454g_d)

§ the cost of carbon black presented in this publication is only an approximation based on 1993 prices. It does not represent the actual cost of carbon black which will fluctuate according to a number a factors.

¶ Table 1 is only a measure of performance for different grades of carbon black and should not be considered an endorsement for any particular product or carbon black manufacturer.